

Supporting information

Table S1: XPS C 1s Spectra Fitting in **Figure S3**

sp ²	sp ³	C-O	C-O-C	C=O	COOH	pi-pi*
284.6	285.4	286.5	287.62	288	288.7	290.99

*All units = eV

Table 2. Raman Vibrational Map of the Composite*

Fc	LRGO/Fc	Vibration assignment
395	415	Cp ring; tilt
855	850	C-H; bend
1104	1160	Cp ring breathing
1396	1406	C-C; stretch

* All units = cm⁻¹

The C-H bending modes of the Cp ring are also sensitive to electrostatic effects. Consistent with our interpretation of the peak's shifts, the increasing positive charge on the Cp ring leads to increased force constants. This trend is consistent with the observed downshift (i.e. lower force constant) of the Cp C–H bending mode from 855 to 850 cm⁻¹, since interaction with the conducting carbon effectively decreases the natural positive charge on the ring itself.

The changes in carbon-related peaks are much more insignificant as follows: D-band: 1320 to 1232, G-band: 1586 to 1590, D'-band: 2660 to 2664 cm⁻¹.

Optimization of LRGO. To optimize the LRGO production, many parameters were tested including: the concentration of GO in slurry, the substrate, the air flow during drying step, the heat rate and more. **Figure S1** presents the effects of three parameters, namely the laser power, the number of irradiation repetitions and the number of GO layers cast onto the substrates based on two important features of the product: (1) the sample conductivity and (2) the mass loss. In the figure, each layer, highlighted with different background colors, was irradiated three times. Four laser powers were tested (10, 12, 14 and 16 W).

The data for sample conductivity shows an increase in conductivity (a decrease in recorded resistance) for every additional laser treatment. This is a result of a higher level of de-oxygenation and graphitization, indicated by the spectroscopy experiments (**Figure 3**). One exception is the first layer, however, the

conductivity of the samples irradiated at high power (14 and 16 W) actually decrease. This is a direct result of the massive mass loss (see **Figure S2b**), as the laser creates holes in the sample that impedes the electrical pathway. When more layers of GO thicken the sample, the holes are filled in with conducting material and the conductivity increases.

The mass loss presented in **Figure S2b** reveals the disadvantage of utilizing high laser powers as large portion of the sample simply vanish. The trade-off between conductivity and mass maintenance is an example of how careful one should be when Applying the reducing process to convert GO into rGO.

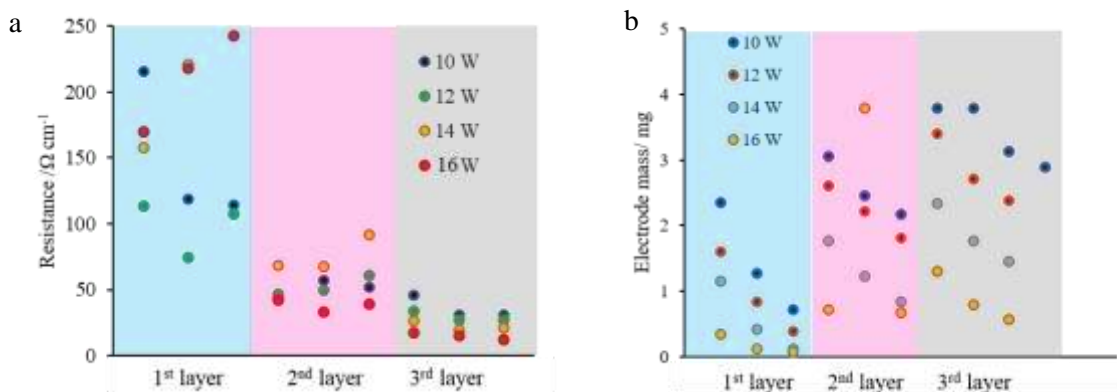


Figure S1. Physical impact of the laser power and the number of GO layers on LRGO.

a. Electrical conductivity calculated using a two-probe voltmeter. b. Mass loss calculated by direct measurement of the sample mass before and after laser treatment.

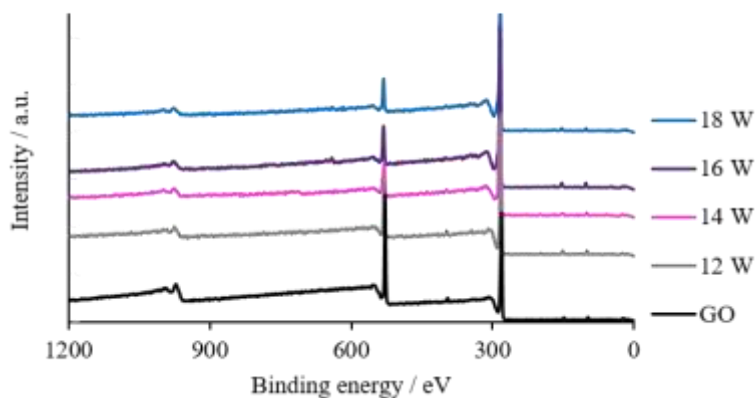


Figure S2. XPS spectrum of GO and LRGO converted with different laser powers.

Fitting of the C 1s peak. A standard XPS response of the C 1s orbital is at binding energies of 282-290 eV. The peak consists of different types of carbon bonds that can be distinguished by their peak position. The

peaks are often too close and are not separate one from the other, hence, require peak fitting according to the shape of the recorded peak is required. For the sake of consistency, the fitting of all spectra were carried out using the same components, as listed in **Table S1**.

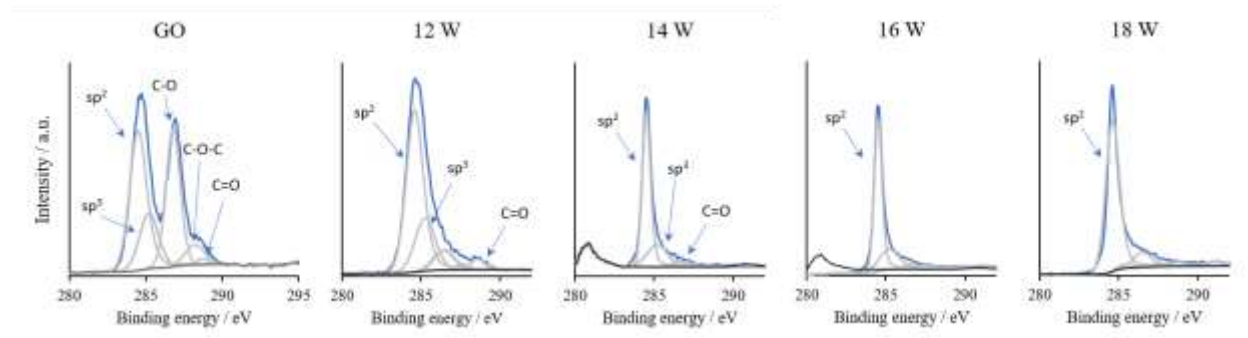


Figure S3. XPS spectra of C 1s. Fitting of peak area was done based on the positions indicated in **Table S1**.

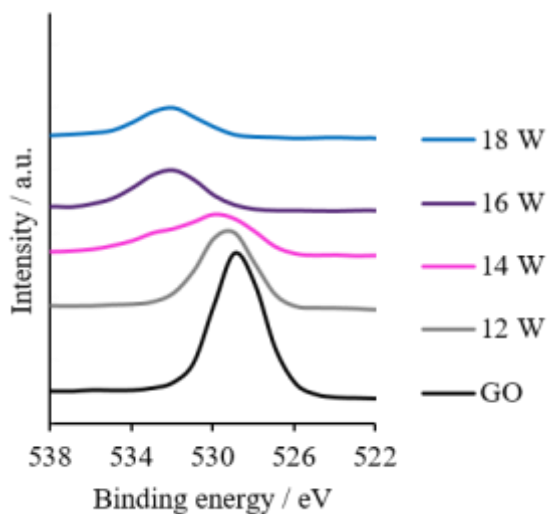


Figure S4. XPS spectra of O 1s for GO and LRGO converted at different laser power.

Raman analysis of the effect of laser power in the graphitization process. The first indication for the laser impact on graphitization is obtained from the shape of the D- and G- bands that are both broadened for the highly oxidized graphene-oxide sample and become sharper as the laser treatment becomes more intense.

The D-band at 1334 cm^{-1} is a result of resonance induced by defects in the graphene structure, while the G-band at 1580 cm^{-1} , which arises from the stretching of the C-C bond in graphitic materials, is a fundamental indicator for the graphitic nature of the carbon.

The G'-band is also known as the 2D-band. This band is a second-order two-phonon process, originating from the resonance between two graphene layers, and provides an accurate indication for the degree of graphitization. The G'-band does not appear in the spectrum of the GO sample nor in the spectrum of LRGO irradiated at low power ($<14\text{ W}$). In contrast, at increased power, the G'-band becomes increasingly dominant until at 18 W it becomes the most intense peak.

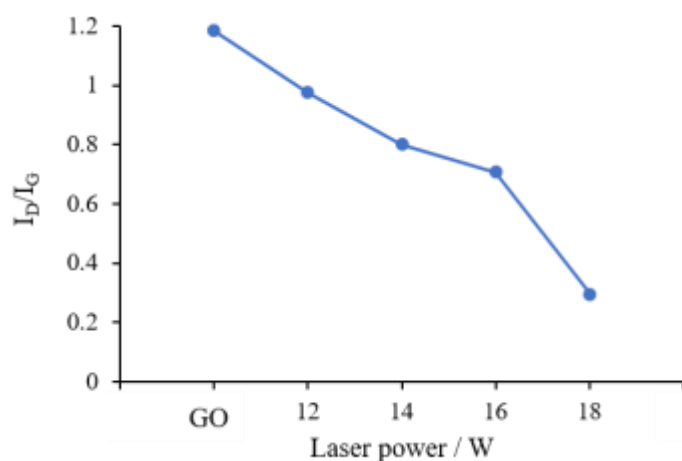


Figure S5. I_D/I_G ratio Raman spectroscopy of LRGO obtained at different laser powers.

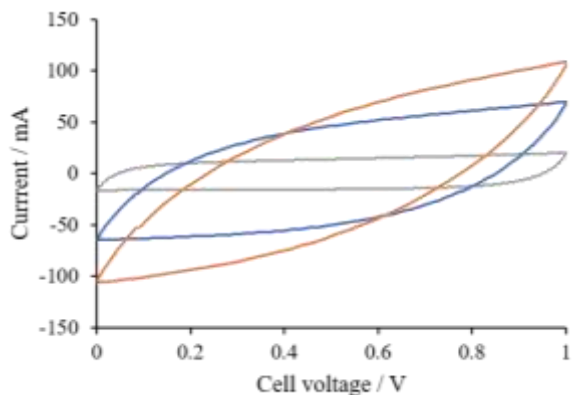


Figure S6. Cyclic voltammogram of LRGO at scan rate of $1, 5$ and 10 V s^{-1} .

The LRGO performances were evaluated by galvanostatic constant current experiments. The graph at the lowest current density demonstrate a virtually ideal linear curve. The capacitance obtained from this measurement is 79 F g^{-1} . At moderate current density of 5 A g^{-1} the shape of the galvanistatic curve become

a little distorted and the capacitance slightly decrease to 71 F g^{-1} . At very high currents, the IR capacitance is reduced by another 30% and the IR drop is more pronounced, although the general shape of the curve remains triangular. The resistance calculated from IR drop of 1 A g^{-1} curve is as little as 3.75Ω .

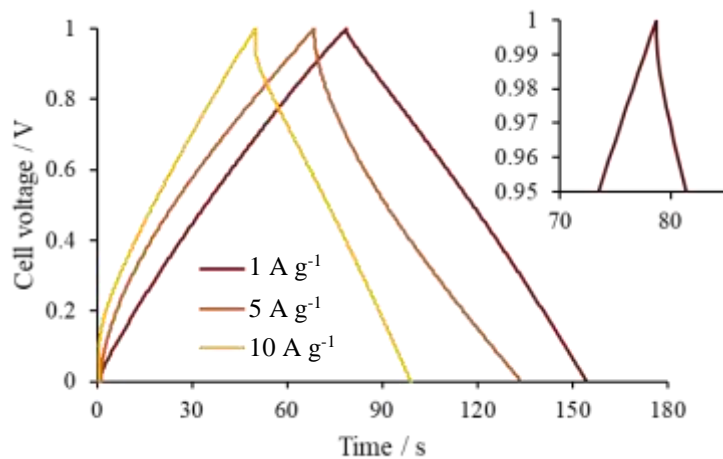


Figure S7. Galvanostatic charge/discharge of LRGO at current densities of 1, 5 and 10 A g^{-1} . Inset: IR drop obtained from galvanostatic curve at 1 A g^{-1} .

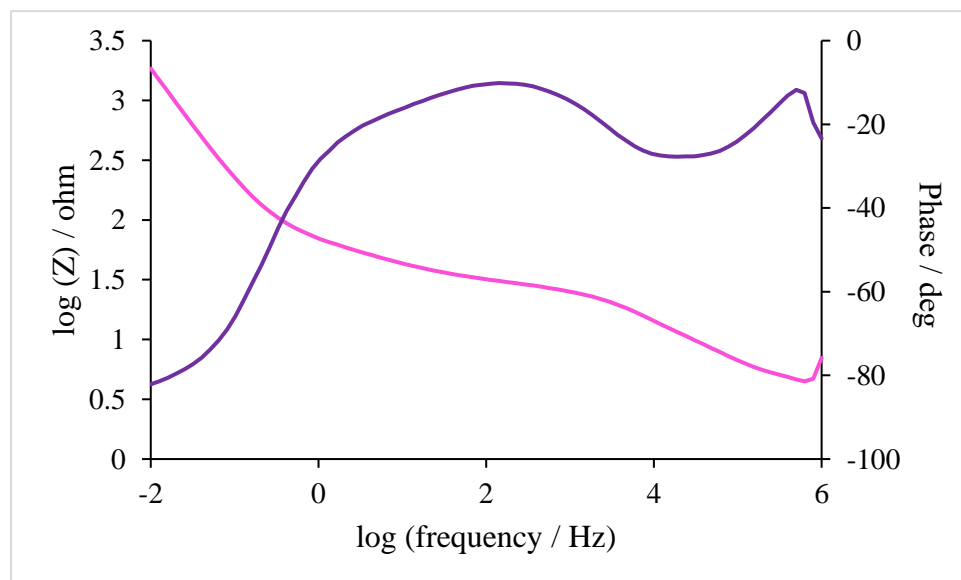


Figure S8. Bode plot for a commercial activated carbon.

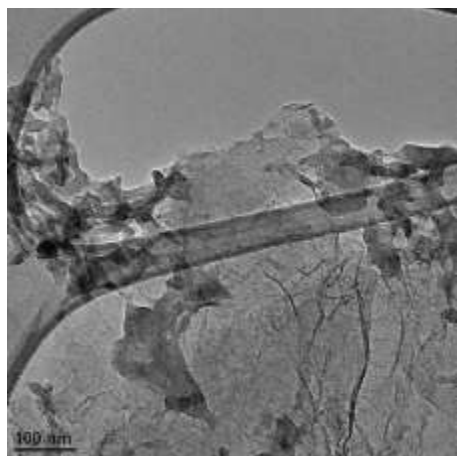


Figure S9. TEM image of LRGO/ferrocene obtained by the wet adsorption method.

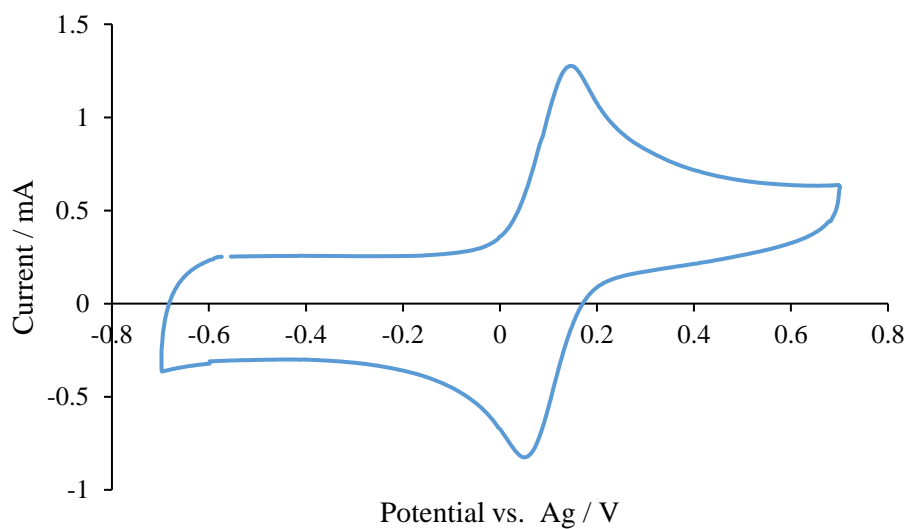


Figure S10. Cyclic voltammogram of 0.01 M ferrocene dissolved in 1 M TEABF₄ in acetonitrile. The scan rate was 20 mV s⁻¹. A platinum wire served as both the working and counter electrodes and the reference electrode was Ag/Ag⁺.

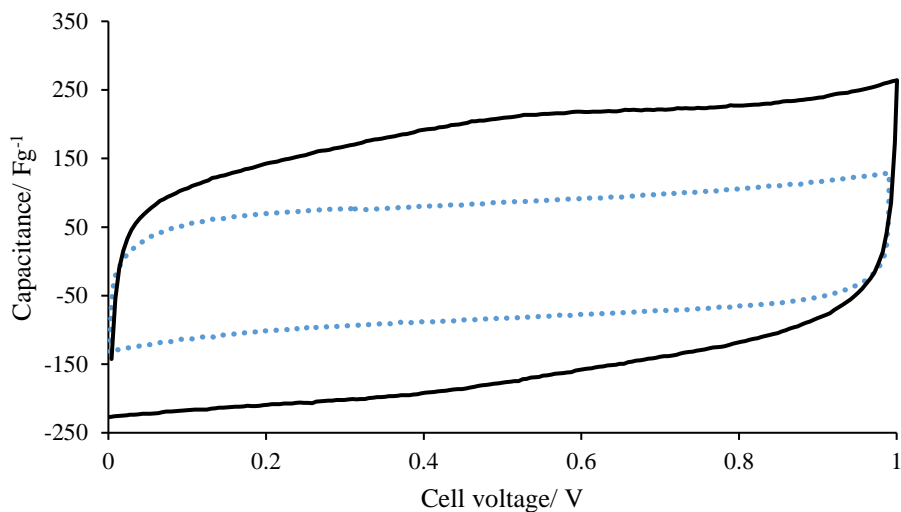


Figure S11. Electrochemical comparison of the LRGO/fc composite (black curve) and LRGO (blue curve). The cell consisting of mass-balanced composite electrodes demonstrates an increase of 196% in specific capacitance compares to a cell comprised of symmetric reduce graphene oxide electrodes. The scan rate was 20 mV s^{-1} . The shape of the composite is only slightly changed from the typical rectangular shape of pure EDL capacitance since the two-electrode coin cell configuration blurs the sharp redox peaks of the active material.